Genes to Cells

Dickkopf 3 attenuates xanthine dehydrogenase expression to prevent oxidative stress-induced apoptosis

Shuang Qui, Junko Kano* and Masayuki Noguchi

Department of Diagnostic Pathology, Faculty of Medicine, University of Tsukuba, Tsukuba, Ibaraki 305-8575, Japan

Dickkopf (DKK) 3 is a DKK glycoprotein family member that controls cell fate during embryogenesis and exerts opposing effects on survival in a cell type-dependent manner; however, the mechanisms governing its pro-apoptosis versus pro-survival functions remain unclear. Here, we investigated DKK3 function in Li21 hepatoma cells and tPH5CH immortalized hepatocytes. *DKK3* knockdown by siRNA resulted in reactive oxygen species accumulation and subsequent apoptosis, which were abrogated by administration of the antioxidant N-acetyl-cysteine. Moreover, forced *DKK3* over-expression induced resistance to hydrogen peroxide (H_2O_2)-induced apoptosis. Expression analysis by cDNA microarray showed that xanthine dehydrogenase (*XDH*) expression was significantly lower in Li21 and tPH5CH *DKK3*-over-expressing cells in response to H_2O_2 treatment when compared to that in their respective mock-transfected controls, whereas a marked increase was observed in H_2O_2-treated *DKK3* knockdown cells. Thus, these data suggest that DKK3 promotes cell survival during oxidative stress by suppressing the expression of the superoxide-producing enzyme XDH.

Introduction

Dickkopf (DKK) 3 is a member of the evolutionarily conserved DKK family of secreted glycoproteins known to antagonize Wnt signaling by binding the Wnt receptor complex, low-density lipoprotein receptor-related protein 5/6 and Kremens (Mao *et al.* 2001; Wang *et al.* 2008). Based on DNA sequence similarity and its location on a paralogous chromosome, DKK3 is thought to be a divergent family member, although its functional significance in Wnt signaling remains ill-defined (Krupnik *et al.* 1999; Guder *et al.* 2006; Niehrs 2006). In addition, DKK family members control cell fate in a coordinated manner (Suwa *et al.* 2003; Diep *et al.* 2004; Fjeld *et al.* 2005; Nie 2005). In some normal adult organs —such as the pancreas, retina, prostate and gastrointestinal tract, DKK3 is expressed by specific cell subpopulations with putative stem-like properties, where it can promote cell survival in a cell type-dependent manner (Byun *et al.* 2005; Kawano *et al.* 2006; Hermann *et al.* 2007; Nakamura *et al.* 2007). We previously showed that DKK3 is differentially expressed in adult porcine hepatic stem-like cells and up-regulated in the early fetal liver, as well as in the regenerating adult liver in an 80% hepatectomy model, supporting its functional relevance to hepatic development (Kano *et al.* 2008). Collectively, these results suggest that DKK3 participates in development, differentiation and survival throughout the vertebrate lifespan, albeit through an undescribed mechanism.

The WNT/β-catenin pathway plays an important role in tumorigenesis, and accumulated data suggest the involvement of DKKs as Wnt antagonists in various malignancies (Kawano & Kypta 2003; Niehrs 2006; Veeck & Dahl 2012). *DKK3* is down-regulated by aberrant hypermethylation in several cancers, where its subsequent forced expression induces tumor suppression and apoptosis (Kobayashi *et al.* 2002; Hoang *et al.* 2004; Roman-Gomez *et al.* 2004; Abarzua *et al.* 2005). Therefore, it has been reported that DKK3 acts as a tumor suppressor and is a potential therapeutic target (Kobayashi *et al.* 2002; Sato *et al.* 2007; Koppen *et al.* 2008; Veeck *et al.* 2008; Yue *et al.* 2008; Veeck & Dahl 2012). However, recent studies support that DKK3 may have a more variable function in certain tumor types. For instance, DKK3 is up-regulated in hepatoblastomas (HBLs) and hepatocellular carcinomas (HCCs) (Pei *et al.* 2009) and can promote cell

Communicated by: Kohei Miyazono
**Correspondence:* junkano@md.tsukuba.ac.jp

DOI: 10.1111/gtc.12484

© 2017 Molecular Biology Society of Japan and John Wiley & Sons Australia, Ltd

migration and dedifferentiation in head and neck squamous cell carcinomas and pancreatic cancer (Zenzmaier *et al.* 2012; Katase *et al.* 2013). Moreover, *DKK3* is reported to protect lung adenocarcinoma cells from oxidative stress and apoptosis, despite only modest expression owing to promoter methylation (Jung *et al.* 2010). Thus, its variable expression and broad range of context-dependent effects indicate that DKK3 could be a promising target for the treatment of certain malignant tumors.

The aim of this study was to clarify the function of DKK3 and its mechanism of action in DKK3-expressing cells. Notably, we showed that DKK3 promotes cell survival by suppressing XDH expression, thereby limiting reactive oxygen species (ROS) accumulation and subsequent apoptosis.

Results

DKK3 suppression induces apoptosis and mitochondrial membrane depolarization in Li21 and tPH5CH cells

We first examined DKK3 expression in fifteen cell lines, of which ten expressed DKK3 mRNA and protein at various levels (Fig. 1A,B). From this, we decided to use the Li21 hepatoma cell line and tPH5CH immortalized hepatocytes because of their considerable expression level and ease of use. Thus, Li21 and tPH5CH cells were transfected individually with three different small interfering RNAs targeting *DKK3* (siDKK3) and knockdown at the mRNA and protein level was confirmed 48 h after transfection (Fig. 2A,B, Fig. S1 in Supporting Information). Notably, *DKK3*-knockdown cells initially attached to the culture surface, but gradually detached over time (Fig. 2C). Cell counting analysis and WST-1 assays showed that proliferation of siDKK3-transfected cells was significantly suppressed relative to that of the negative control (siCtr) group (Fig. 2D,E). To evaluate the effect of *DKK3* knockdown on apoptosis, caspase 3/7 activity, phosphatidylserine (PS) exposure on the outer plasma membrane and mitochondrial membrane depolarization were assessed. Caspase 3/7 activity was significantly higher in siDKK3-transfected cells than in siCtr controls at 48 h after siRNA transfection (Fig. 2F). Moreover, PS exposure markedly increased in siDKK3-transfected cells and was accompanied by significantly lower JC-1 staining when compared to that in siCtr controls, indicative of apoptotic cells with mitochondrial depolarization (Fig. 2G,H).

Increased ROS in *DKK3*-knockdown cells

Mitochondrial membrane depolarization is a crucial event during apoptosis that can be induced by both the intrinsic and extrinsic cell death pathways. Major intrinsic apoptotic stimuli include severe cellular stressors, such as UV and gamma radiation, ROS and heat. Analysis with the fluorescence marker CellROX showed that ROS levels were approximately twofold and sixfold higher in siDKK3 cells when compared to that in siCtr controls 14 and 24 h after siRNA

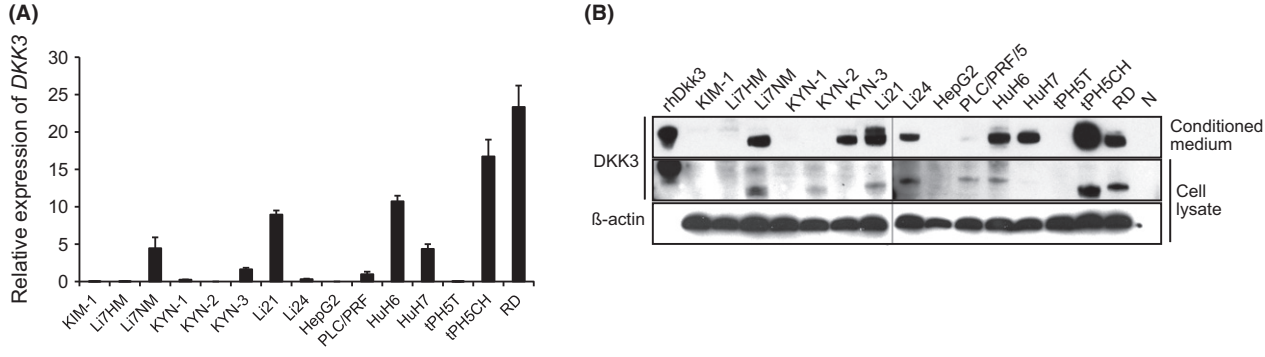

Figure 1 DKK3 expression in human cell lines. (A) *DKK3* mRNA expression was normalized that of 18S ribosomal RNA in real-time PCR analysis. (B) DKK3 protein levels were assessed by immunoblotting 10 or 40 μg protein from conditioned medium or cell lysates, respectively, after culturing for 24 h. β-actin was used as a loading control. Recombinant human DKK3 protein produced by a mouse myeloma cell line (rhDKK3) and sterilized water were used as positive and negative (N) controls, respectively. Hepatocellular carcinoma (HCC) cells lines: KIM-1, Li7HM, Li7NM, KYN-1, KYN-2, KYN-3, Li21, PLC/PRF/5, HuH7, tPH5T; Hepatoblastoma (HBL) cell lines: Li24, HepG2, HuH6; immortalized human non-neoplastic hepatocyte cell line: tPH5CH; fetal-type rhabdomyosarcoma cell line: RD.

© 2017 Molecular Biology Society of Japan and John Wiley & Sons Australia, Ltd

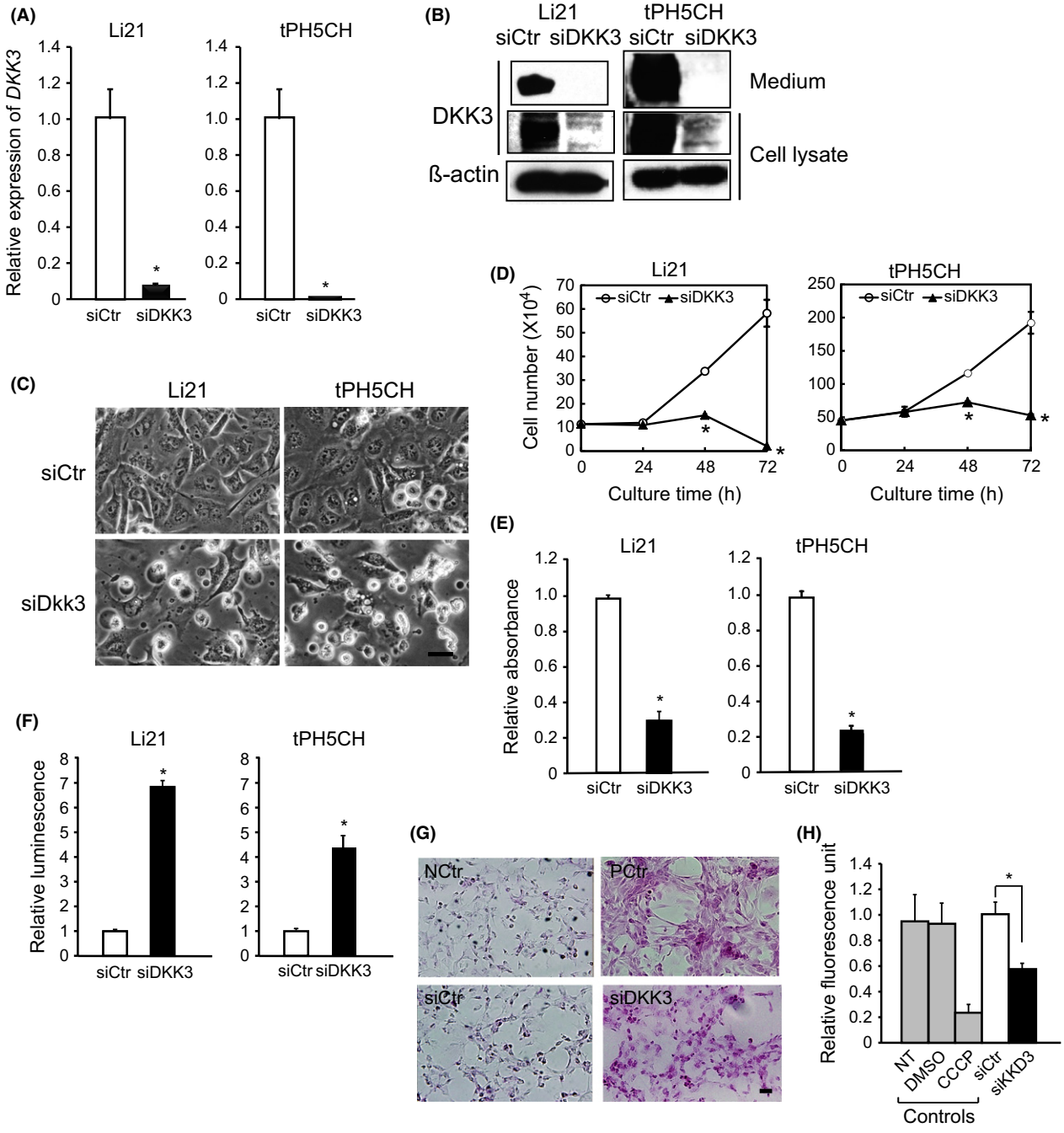

Figure 2 Induction of apoptosis in Li21 and tPH5CH *DKK3*-knockdown cells. (A) *DKK3* mRNA levels were analyzed by real-time PCR 48 h after siRNA transfection. (B) DKK3 protein knockdown confirmed by Western blot analysis 48 h after siRNA transfection. β-actin was used as a loading control. (C) Phase-contrast micrographs of cells 48 h after siRNA transfection. (D) Attached cells were counted using a hemocytometer. (E) Cell proliferation was assessed 48 h after siRNA transfection by WST-1 assay. (F) Caspase 3/7 activity was measured 48 h after siRNA transfection. (G) PS exposure was detected with the Cell-APOPercentage Apoptosis Assay 48 h after siRNA transfection in Li21 cells. PCtr, positive control; siCtr, siRNA control; NCtr, non-treated control. (H) Mitochondrial membrane depolarization was monitored 48 h after *DKK3*-knockdown by JC-1 staining in Li21 cells. Scale bars, 50 μm; $*P < 0.05$.

 © 2017 Molecular Biology Society of Japan and John Wiley & Sons Australia, Ltd

transfection, respectively; however, no notable difference was observed in the presence of N-acetyl-cysteine (NAC) (Fig. 3A). Furthermore, several nuclei with strong fluorescence were observed in the siDKK3-transfected and menadione-treated (positive control) groups, but few were evident in siCtr- and NAC-treated counterparts (Fig. 3B). A similar effect was observed in proliferation analyses, where NAC treatment rescued the diminished proliferation of siDKK3 cells at 48 and 72 h post-transfection (~1.3- and ~1.7-fold increase, respectively) (Fig. 3C). Moreover, phase-contrast microscopy showed that the majority of cells remained adherent in the presence of 4.0 mM NAC, whereas several round and floating cells were observed in the untreated control group (Fig. 3D).

DKK3 over-expression confers increased resistance to H_2O_2-induced oxidative stress

We next examined whether DKK3 over-expression increased the resistance to H_2O_2-induced oxidative stress in Li21 and tPH5CH cells. Real-time PCR and Western blotting confirmed DKK3 over-expression at the mRNA and protein level in $Li21^{DKK3}$ and $tPH5CH^{DKK3}$ cells compared to that in mock-transfected controls ($Li21^{Mock}$ and $tPH5CH^{Mock}$ cells)

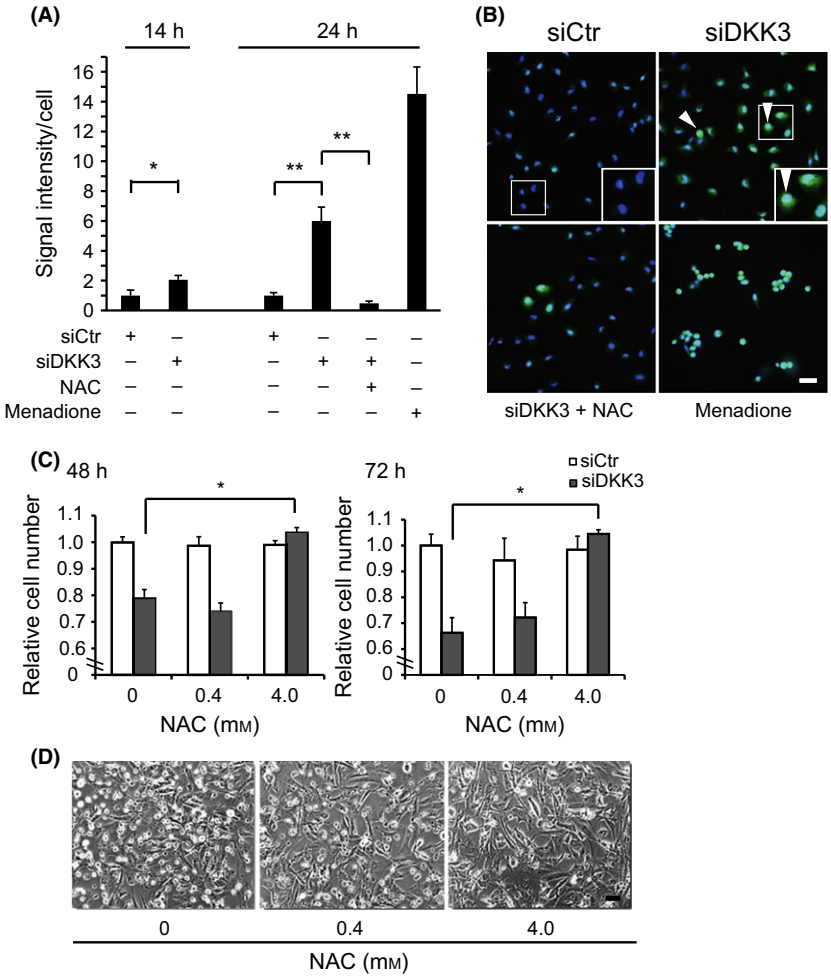

Figure 3 ROS accumulation in *DKK3*-knockdown cells. (A) ROS accumulation was measured by CellROX green staining at 14 and 24 h after siRNA transfection following treatment with N-acetyl-cysteine (NAC, 4.0 mM) or menadione (100 μM). (B) Representative fluorescence microscopy images of Li21 cells 24 h after siRNA transfection. ROS (green, white arrowheads); nuclei (blue). (C) siRNA-transfected cells were treated with increasing concentrations of NAC (0, 0.4 and 4.0 mM) and counted 48 (left) or 72 h (right) later. (D) Cell morphology and adherence were assessed by phase-contrast microscopy 48 h after siRNA transfection. Scale bar, 50 μm; $*P < 0.05$, $**P < 0.01$.

© 2017 Molecular Biology Society of Japan and John Wiley & Sons Australia, Ltd

(Fig. 4A,B). Notably, $Li21^{DKK3}$ and $tPH5CH^{DKK3}$ cells were more resistant to all concentrations of H_2O_2 (Fig. 4C, Figs S2 and S3 in Supporting Information) and retained their characteristic adherence and spread morphology in the presence of 500 and 400 μM H_2O_2, respectively (Fig. 4D).

DKK3 suppresses *XDH* expression during oxidative stress

To investigate the mechanism responsible for the protective effects of DKK3 during oxidative stress, expression of the redox enzymes superoxide dismutase 1/2 (*SOD1/2*), heme oxygenase 1 (*HMOX1*), glutathione synthase (*GSS*) and catalase (*CAT*) was examined in siDKK3- and siCtr-transfected Li21 cells, but no significant differences were observed (Table S1, and Figs S4 and S5 in Supporting Information). Similarly, no marked changes were found in the expression or activities of nicotinamide-adenine dinucleotide phosphate oxidases (also known as NOX enzymes) (Fig. S6). Thus, cDNA microarrays were used to evaluate differential gene expression in $Li21^{DKK3}$ and $tPH5CH^{DKK3}$ cells with and without

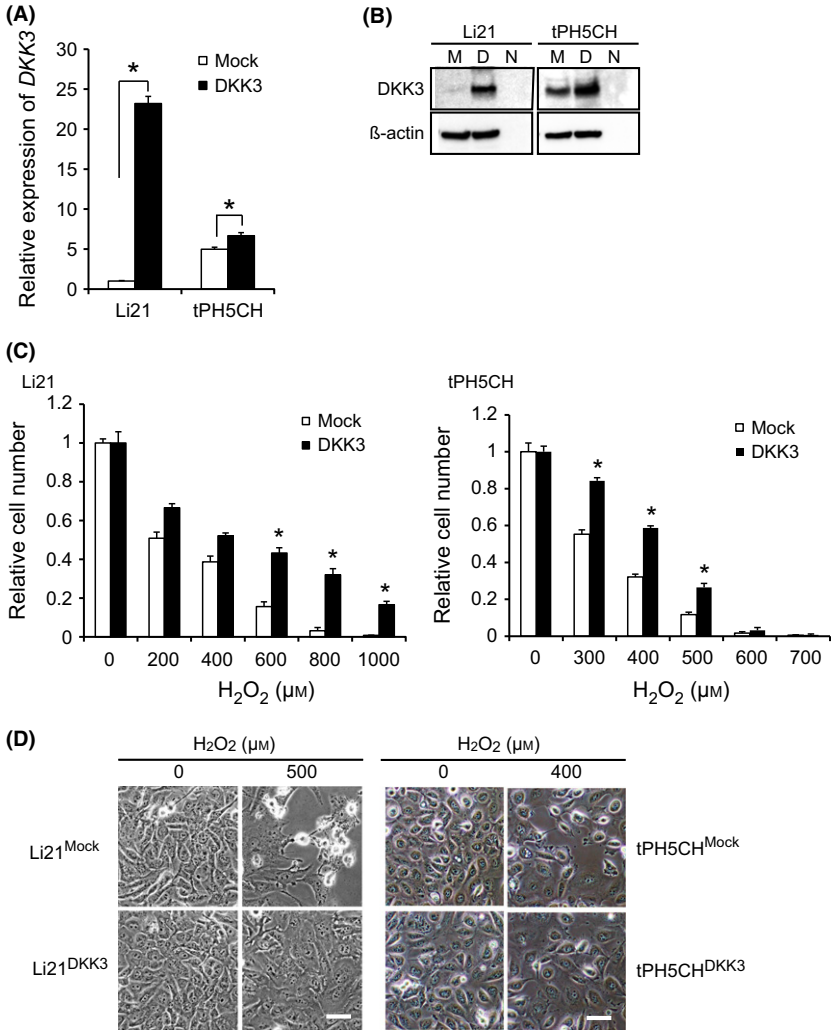

Figure 4 *DKK3* over-expression increases resistance to H_2O_2-induced oxidative stress in Li21 and tPH5CH cells. (A, B) Forced DKK3 over-expression was confirmed in Li21 and tPH5CH cells at the (A) mRNA and (B) protein levels. D, *DKK3*-transfected cells; M, mock-transfected cells; N, negative control. (C) *DKK3*- and mock-transfected cells were cultured for 24 h before treatment with increasing concentrations of H_2O_2 (0–1000 μM). Cells were counted 18 h later. (D) Phase-contrast microscopy of siDKK3- and mock-transfected Li21 and tPH5CH cells 18 h after treatment with 500 and 400 μM H_2O_2, respectively. Scale bar, 50 μm; $^*P < 0.05$ vs. mock-transfected controls.

 © 2017 Molecular Biology Society of Japan and John Wiley & Sons Australia, Ltd

H_2O_2 treatment, which showed 12210 and 9973 differentially expressed genes in Li21 and tPH5CH cells, respectively. Of these, 4180 genes showed similar expression changes in the two cell lines (Table S2). Notably, the enzyme XDH was substantially down-regulated in response to H_2O_2 (0.49- and 0.46-fold change in Li21 and tPH5CH cells, respectively) (Table 1). Further analysis by real-time PCR indicated that H_2O_2 treatment induced 6.2- and 1.2-fold higher *XDH* expression in mock- and siDKK3-transfected Li21 cells, respectively, with a similar effect observed in tPH5CH cells (7.9- and 5.4-fold increases in mock- and siDKK3-transfected cells, respectively). Thus, *XDH* expression was markedly lower in *DKK3* over-expressing cell lines (Fig. 5A). The functional significance of DKK3 in H_2O_2-induced *XDH* expression changes was determined using the experiment described in Fig. 5B, which showed a significantly more pronounced up-regulation in Li21 and tPH5CH *DKK3*-knockdown cells (Fig. 5C). To confirm this finding, we examined whether *XDH* siRNA knockdown suppressed H_2O_2-induced toxicity in Li21 and tPH5CH cells. As expected, siXDH cells treated with H_2O_2 24 h post-transfection showed a significantly higher viability than siCtr-transfected controls did (Fig. 6A). In addition, siDKK3 cells showed increased *XDH* mRNA expression and cell death 48 h after transfection as compared to that reported for siDKK3/siXDH cotransfectants (Fig. 6B–D). Collectively, these data suggest that *DKK3* attenuates H_2O_2-induced *XDH* expression.

Table 1 Differentially expressed genes following H_2O_2 treatment in Li21 and tPH5CH cells (defined as ≥2 and ≤0.5 for up- and down-regulated genes, respectively)

		DKK3(H_2O_2/Ctr)-Mock(H_2O_2/Ctr)	
Gene	Accession No.	Li21	tPH5CH
CXCL1	NM_001511	5.156	1.393
PAPLN	NM_173462	2.727	−0.035
AREG	NM_001657	2.394	−0.497
WNT5A	NM_003392	2.394	−0.497
EGEG	NM_001432	2.206	−0.625
ZNF469	NM_001127464	2.072	−1.242
IL6	NM_000600	1.192	−2.323
LINC01270	NR_034124	1.075	1.162
LOC344887	NR_033752	0.678	−2.394
BEX2	NM_001168399	0.508	−2.750
PADI1	NM_013358	−0.303	2.154
XDH	NM_000379	−1.039	−1.122
EGR1	NM_001964	−1.85	−1.080
FAM167B	NM_032648	−2.022	−0.070
DSEL	NM_032160	−2.162	0.644

Expression values are log2-transformed.

Discussion

In this study, we showed that DKK3 promotes cell survival by attenuating expression the pro-oxidant XDH and subsequent ROS accumulation. In malignant cells, DKK3 can function as either a tumor-suppressor gene or oncogenic factor depending on cell type and context (Zenzmaier *et al.* 2013). Moreover, several reports have described increased DKK3 expression in tumor-associated cells, such as stromal and endothelial cells, where it appears to support differentiation and tissue remodeling and is associated with a favorable prognosis (St Croix *et al.* 2000; Untergasser *et al.* 2008; Fong *et al.* 2009; Muhlmann *et al.* 2010; Zenzmaier *et al.* 2013). These data suggest that DKK3 plays a distinct and complex role in cancer cell survival, differentiation and apoptosis.

The present study examined DKK3 function in Li21 hepatoma cell line (Ishiyama *et al.* 2003). Notably, *DKK3* suppression by siRNA knockdown induced apoptosis, suggesting that it acts as a pro-survival factor in this cell type. A previous report on lung adenocarcinoma identified ROS accumulation as a possible pro-apoptotic stimulus following *DKK3* suppression (Jung *et al.* 2010), similar to that observed in our study. Moreover, our microarray and functional analyses showed that *DKK3*-mediated *XDH* suppression is likely responsible for this result in both Li21 hepatoma cells and tPH5CH immortalized hepatocytes, suggesting that this effect was not caused by oncogenic mutation. This was further supported by a rescue study demonstrating that *XDH* suppression was associated with H_2O_2-induced toxicity in Li21 and tPH5CH cells. These findings may result from production of the strong antioxidant uric acid (Fig. 6A). Interestingly, siDKK3 cells showed increased *XDH* mRNA expression, whereas siDKK3/siXDH cotransfected cells exhibited increased viability, suggesting *XDH* expression was involved in the pro-survival function of DKK3 (Fig. 6B–D). However, the spontaneous increase in *XDH* mRNA expression in siDKK3-transfected cells appears to be difficult to detect because of a concomitant induction of cell death.

XDH is a molybdopterin-flavin enzyme that catalyzes the final steps of purine catabolism (Battelli *et al.* 2014a) and exists as two isoforms—dehydrogenase and

© 2017 Molecular Biology Society of Japan and John Wiley & Sons Australia, Ltd

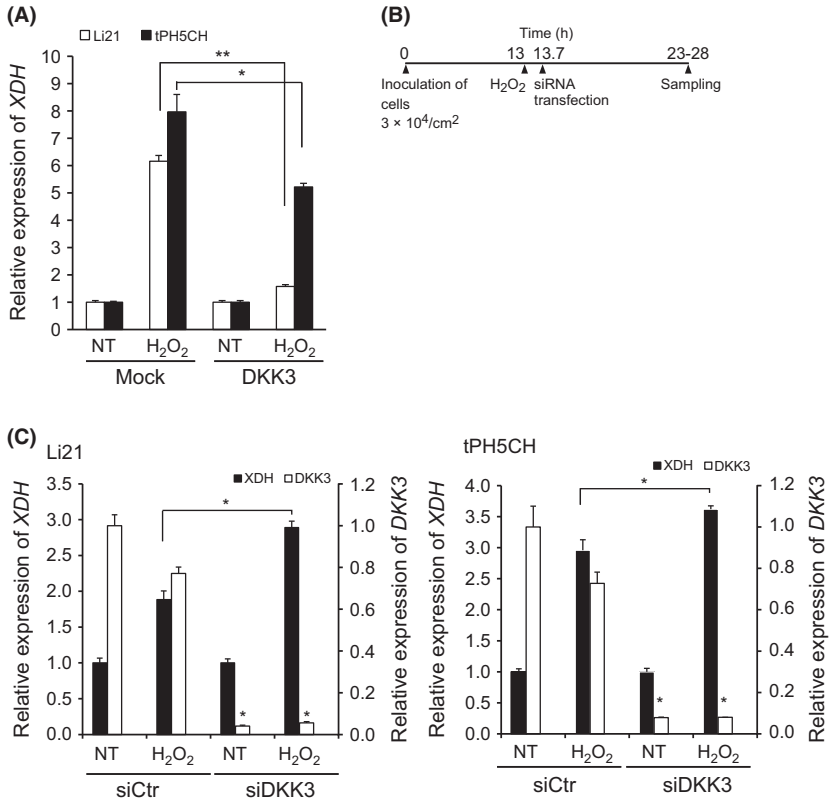

Figure 5 Increased xanthine dehydrogenase (XDH) expression in *DKK3*-knockdown cells following H_2O_2 treatment. (A) *XDH* mRNA expression was monitored in siDKK3- and mock-transfected Li21 and tPH5CH cells before and after H_2O_2 treatment. (B) Procedural schematic XDH expression analysis following H_2O_2 treatment in siRNA-transfected cells. (C) *XDH* and *DKK3* mRNA expression analysis in Li21 and tPH5CH cells transfected with siDKK3 or control siRNA (siCtr). NT, nontreated; $*P < 0.05$, $**P < 0.01$.

oxidase—with antioxidant and prooxidant effects, respectively. Thus, XDH likely functions to tightly control cellular redox status. *XDH* expression is regulated at very low levels in humans and some anthropoid apes through an ill-defined mechanism and has been implicated in many pathological conditions—such as gout, heart disease, reperfusion injury and hypertension, suggesting that it may be an effective therapeutic target (Nishino *et al.* 1997; Xu *et al.* 2000, 2004; Agarwal *et al.* 2011; Battelli *et al.* 2014a,b, 2015; Khambata *et al.* 2015). Here, our results support a model in which DKK3 suppresses XDH expression in response to oxidative stress, thereby protecting cells from the excess ROS produced by XDH activation. However, it is not clear whether XDH is the only driver of oxidative stress in the absence of DKK3 (Fig. 6E) or if this function is associated with DKK3's role in organogenesis and differentiation. Alternatively, secreted DKK3 (Fig. 1) may also regulate the global redox environment and thereby modify the activity of other secreted antioxidants—such as glutathione—via thiol-disulfide exchange. Thus, further studies are required

Figure 6 *XDH* suppression enhanced cell viability following H_2O_2 treatment and in *DKK3*-knockdown cells. (A) siXDH- and siCtr-transfected cells were cultured for 24 h before treatment with increasing concentrations of H_2O_2 (0–800 μM). Cell viability was assessed 10 h later. (B) Real-time PCR analysis of *XDH* expression 48 h after siDKK3 transfection in Li21 and tPH5CH cell lines compared to siCtr-transfected controls. (C) Cell viability was monitored in Li21 and 5CH cells 48 h after transfection with both siDKK3 and siXDH or siDKK3 alone. (D) Phase-contrast microscopy of siDKK3-, siXDH- and siCtr-transfected Li21 and tPH5CH cells 48 h after transfection. (E) Proposed model of DKK3 activity. Scale bar, 50 μm; $*P < 0.05$ vs. siCtr-transfected controls.

 © 2017 Molecular Biology Society of Japan and John Wiley & Sons Australia, Ltd

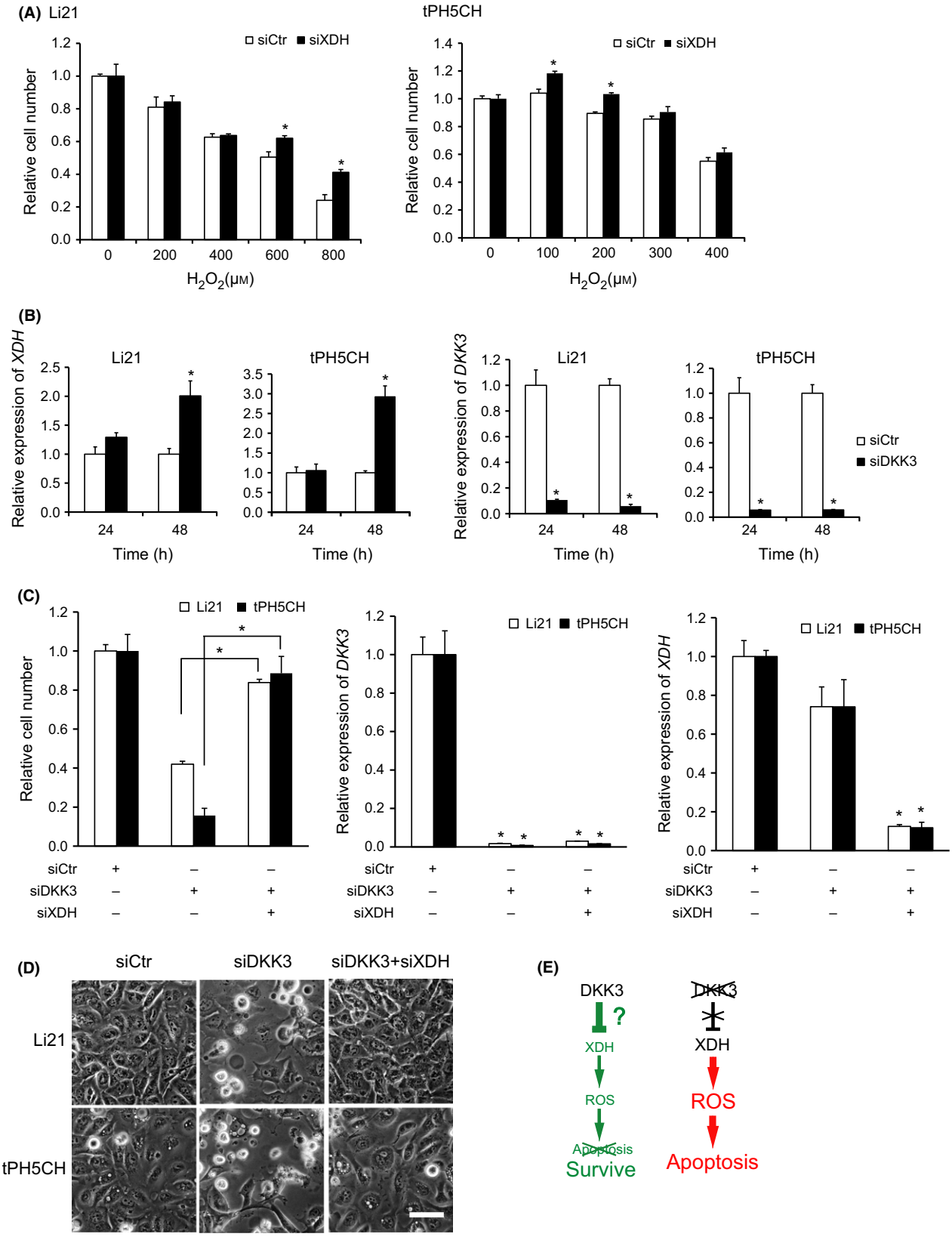

© 2017 Molecular Biology Society of Japan and John Wiley & Sons Australia, Ltd

to clarify the mechanism of DKK3-dependent *XDH* suppression in response to oxidative stress.

In conclusion, we showed that DKK3 promotes cell survival during oxidative stress by suppressing *XDH* expression, thereby abrogating excess ROS accumulation and subsequent apoptosis. Whereas the exact mechanism by governing this process remains to be fully elucidated, these data support the potential significance of DKK3 as a clinically relevant target for the treatment of diseases characterized by chronic oxidative stress.

Experimental procedures

Cell culture

Ten established human HCC cell lines (KIM-1, Li7HM, Li7NM, KYN-1, KYN-2, KYN-3, Li21, PLC/PRF/5, HuH7 and tPH5T), three HBL cell lines (Li24, HepG2 and HuH6), a rhabdomyosarcoma cell line (RD) and an immortalized human non-neoplastic hepatocyte cell line (tPH5CH) were analyzed for DKK3 expression in the cell lysate and culture media. The tPH5T and tPH5CH cell lines were established from tumor and noncancerous tissue isolated from the same patient with chronic hepatitis by transfection with SV-40 large T antigen (Noguchi & Hirohashi 1996) and cultured in a 1:1 mixture of Dulbecco's modified Eagle medium and Ham's F12 medium (Wako, Osaka, Japan) supplemented with 2% fetal bovine serum (FBS, Wako), 120 ng/mL hydrocortisone (Wako), 25 ng/mL epidermal growth factor (Toyobo, Tokyo, Japan), 10 μg/mL transferrin (Sigma-Aldrich, St. Louis, MO, USA), 10 ng/mL selenium (Sigma-Aldrich) and 500 ng/mL linoleic acid (Sigma-Aldrich). RD cells were cultured in Eagle's minimum essential medium with 10% FBS and nonessential amino acids (Sigma-Aldrich), whereas the other cell lines were cultured in RPMI1640 medium containing 5% FBS.

Real-time PCR

Basal *DKK3* mRNA expression was examined in the fifteen cell lines using a Power SYBR Green Cells-to-Ct Kit (Life Technologies, Carlsbad, CA, USA). For other assays, cDNA synthesis was carried out using 1.5–2.0 μg total RNA isolated by RNeasy Plus Mini (QIAGEN, Valencia, CA, USA) per 20 μL of reaction mixture using a High Capacity cDNA Reverse Transcription Kit (Life Technologies). Expression levels were analyzed with Power SYBR Green PCR Master Mix (Life Technologies) and the primers described below. All procedures were conducted in accordance with the manufacturer's protocol. The concentrations and sequences of the forward and reverse primers were as follows: DKK3 (200 μM each): 5′-CACAGACACGAAGGTTGGAAATA-3′, 5′-GACCATTTGTCCAGTCTGGTTG-3′; XDH (200 μM each): 5′-ACCTCAAGTTCTGATGGTGTCTGTC-3′, 5′-GATTCAAGGTTATGCTTTGCTGTTC -3′; 18S ribosomal RNA (100 μM each): 5′-ACTCAACACGGGAAACCTCA-3′, 5′-AACCAGACAAATCGCTCCAC-3′.

Western blot analysis

Cell lysates were extracted using M-PER Mammalian Protein Extraction Reagent (Life Technologies) with 0.1% Triton X-100, separated by SDS-PAGE, and blotted onto polyvinylidene difluoride membranes with an iBlot Gel Transfer Device (Life Technologies). Immunoblotting was carried out according to standard procedures with primary antibodies for DKK3 (goat polyclonal, R&D Systems, Minneapolis, MN, USA) and β-actin (mouse monoclonal, Sigma-Aldrich), and horseradish peroxidase-conjugated anti-goat or anti-mouse IgG secondary antibodies (Life Technologies). Proteins were visualized using SuperSignal West Femto Maximum Sensitivity Substrate (Life Technologies) and BioMax Light Film (Carestream Health, Rochester, NY, USA).

siRNA transfection

Cells were transfected with siRNA (Stealth Select RNA, Life Technologies) targeting *DKK3* (5′-CCUGGCAAACUUACCUCCCAGCUAU-3′), *XDH* (5′-GAACGAGCUUUAUUCCACAUGGACA-3′) or Stealth RNAi Negative Control Duplex (Life Technologies) using Lipofectamine RNAi MAX Reagent (Life Technologies) according to the manufacturer's protocol. Cells were incubated for 24–72 h before use in analyses.

Proliferation assay

Attached cells were dissociated with 0.25% trypsin containing 1 mM EDTA-4Na and counted using trypan blue staining and a hemocytometer. Cells were cultured for 48 h after siRNA transfection, treated with Cell Proliferation Reagent WST-1 (Roche Applied Science, Mannheim, Germany) or Cell Counting Kit-8 (DOJINDO, Kumamoto, Japan) in 10% v/v medium and then incubated for 2 h at 37 °C. The spectrophotometric absorbance of each sample was measured at 450 nm (610 nm reference) with a Varioskan Flash Multimode Reader (Thermo Fisher, Waltham, MA, USA) and analyzed using Skanlt Software (Life Technologies).

Phosphatidylserine (PS) exposure analysis

Cell-APOPercentage dye (Biocolor, Carrickfergus, UK) was used to detect PS exposure on the outside membrane of cells committed to apoptosis according to the manufacturer's protocol. The dye was added to cells 48 h after siRNA transfection. Cells pre-treated with 10 mM H_2O_2 or left untreated were used as positive or negative controls for apoptosis, respectively. Stained cells were fixed with 10% neutralized formalin and photographed with an inverted microscope.

 © 2017 Molecular Biology Society of Japan and John Wiley & Sons Australia, Ltd

Analysis of Caspase 3/7 activity

Caspase 3/7 activity was measured with the Caspase-Glo 3/7 Assay Kit (Promega, Madison, WI, USA). Cells were incubated for 48 h after siRNA transfection, treated with Caspase-Glo 3/7 Reagent and incubated for 30 min at 37 °C. Luminescence was then measured using a TD-20/20 Luminometer (Promega).

Mitochondrial depolarization

Mitochondrial membrane depolarization was assessed using a MitoPT JC-1 Assay Kit (ImmunoChemistry Technologies, Bloomington, MN, USA). Briefly, 48 h after siRNA transfection, cells cultured in a 96-well plate (Nunc, Roskilde, Denmark) were treated with Mito PT JC-1 solution and incubated for 15 min at 37 °C. After washing with Assay Buffer, the cells were resuspended in 100 μL assay buffer per well and measured for relative fluorescence units (RFU) using a Varioskan Flash Multimode Reader (excitation, 490 nm; emission, 527/590 nm). Cells were treated with carbonyl cyanide 3-chlorophenylhydrozone (CCCP) and dimethyl sulfoxide (DMSO) for 75 min before analysis for use as positive and negative controls, respectively.

Measurement of ROS

Cellular oxidative stress was assessed using CellROX Green Reagent (Life Technologies), which allows for the fluorescence-based quantification of ROS. Briefly, cells cultured on collagen-coated coverslips were incubated for 14 and 24 h after siRNA transfection and then stained 5 μM CellROX Green Reagent and 10 μg/mL Hoechst 33342 (Dojindo, Rockville, MD, USA). NAC (4.0 mM) and menadione (100 μM) were added during siRNA transfection or 30 min before the addition of CellROX reagent, respectively. After a subsequent incubation for 30 min at 37 °C, harvested cells were washed three times with Hank's balanced salt solution and fixed with 3.7% neutralized formaldehyde. Fluorescence was measured with a BZ-II Analyzer (Keyence, Osaka, Japan) using 10 randomly selected fields per sample.

NAC administration

Cells cultured in 24-well plates were transfected with siRNA and immediately treated with increasing concentrations of NAC (0, 0.4 and 4.0 mM; Sigma-Aldrich). Cells were then counted after crystal violet staining 48 or 72 h later.

Generation of stable *DKK3*-over-expressing cell lines

The Flexi Vector System (Promega) and mammalian C-terminal FLAG-tagged expression vector pcDNA3-C-FLAG were provided by M. Kato, H. Suzuki and H Watanabe (University of Tsukuba, Ibaraki, Japan) and used to generate Li21 and tPH5CH *DKK3*-over-expressing cell lines. The pFN21AE4338 vector harboring the full-length coding region of human *DKK3* was produced by Kazusa DNA Research Institute and purchased from Promega. The *DKK3* cDNA was shuttled from pFN21AE4338 into pF5KCMV-neo (Promega) to generate the pF5KCMV-DKK3-neo expression vector. For pcDNA-DKK3-C-FLAG, *DKK3* cDNA was PCR-amplified from pFN21AE4338 and subcloned into the EcoRI/XhoI sites of pcDNA3-C-FLAG. Cell lines with stable DKK3 over-expression ($Li21^{DKK3}$ and $tPH5CH^{DKK3}$) were generated by transfection with the pF5KCMV-DKK3-neo or pcDNA-DKK3-C-FLAG plasmids using FuGENE HD Transfection Reagent (Promega), followed by G418 sulfate selection at 200 and 600 μg/mL, respectively. The $Li21^{Mock}$ and $tPH5CH^{Mock}$ cells were generated by transfection with empty vectors and selected as described above.

H_2O_2 treatment

$Li21^{Mock}$, $Li21^{DKK3}$, $tPH5CH^{Mock}$ and $tPH5CH^{DKK3}$ cells were cultured in 24-well plates for 24 h. H_2O_2 was then added at the indicated concentrations, and cells were counted 18 h later.

cDNA microarray analysis

$Li21^{Mock}$, $Li21^{DKK3}$, $tPH5CH^{Mock}$ and $tPH5CH^{DKK3}$ cells were treated with H_2O_2 (800 and 400 μM for Li21 and tPH5CH cells, respectively) for 20 h. Cells treated with sterile water served as paired controls. Total RNA was isolated from treated cells using a QIAGEN RNeasy Plus Mini kit (Qiagen) and assessed for quality with an Agilent Bioanalyzer 2100 (Agilent Technologies, Santa Clara, CA, USA). cDNA microarray analyses were carried out using Agilent G4845A Whole Human Genome Microarray 4 × 44K v2 (Agilent) according to the manufacturer's instructions. Hybridized cDNA microarrays were scanned on an Agilent SureScan Microarray Scanner G2600D, and the images analyzed with Agilent Feature Extraction 11.5 software. Raw probe set intensities were normalized using global normalization algorithm and log2-transformed.

Statistical analysis

Data represent the mean ± standard error of the mean (SE) from at least three independent experiments. Significance was determined with Student's unpaired t-test or one-way ANOVA with Tukey's post hoc tests where appropriate, with $P < 0.05$ considered statistically significant.

Acknowledgements

We gratefully acknowledge Drs Michitaka Ozaki and Sanae Haga for their helpful advice, and Drs Mitsuyasu Kato,

© 2017 Molecular Biology Society of Japan and John Wiley & Sons Australia, Ltd

Hiroyuki Suzuki and Hideyuki Watanabe for gifting the FLAG expression vector. The cDNA microarray analyses were supported by the NIMS Molecule & Material Synthesis Platform of the 'Nanotechnology Platform Project' operated by the Ministry of Education, Culture, Sports, Science and Technology (MEXT), Japan. This work was supported by JSPS KAKENHI Grant Number 21590414.

Author contributions

MN and JK designed the study; SQ and JK carried out the experiments and contributed equally.

References

Abarzua, F., Sakaguchi, M., Takaishi, M., Nasu, Y., Kurose, K., Ebara, S., Miyazaki, M., Namba, M., Kumon, H. & Huh, N.H. (2005) Adenovirus-mediated overexpression of REIC/Dkk-3 selectively induces apoptosis in human prostate cancer cells through activation of c-Jun-NH2-kinase. *Cancer Res.* **65**, 9617–9622.

Agarwal, A., Banerjee, A. & Banerjee, U.C. (2011) Xanthine oxidoreductase: a journey from purine metabolism to cardiovascular excitation-contraction coupling. *Crit. Rev. Biotechnol.* **31**, 264–280.

Battelli, M.G., Bolognesi, A. & Polito, L. (2014a) Pathophysiology of circulating xanthine oxidoreductase: new emerging roles for a multi-tasking enzyme. *Biochim. Biophys. Acta* **1842**, 1502–1517.

Battelli, M.G., Polito, L. & Bolognesi, A. (2014b) Xanthine oxidoreductase in atherosclerosis pathogenesis: not only oxidative stress. *Atherosclerosis* **237**, 562–567.

Battelli, M.G., Polito, L., Bortolotti, M. & Bolognesi, A. (2015) Xanthine oxidoreductase in cancer: more than a differentiation marker. *Cancer Med.* **5**, 546–557.

Byun, T., Karimi, M., Marsh, J.L., Milovanovic, T., Lin, F. & Holcombe, R.F. (2005) Expression of secreted Wnt antagonists in gastrointestinal tissues: potential role in stem cell homeostasis. *J. Clin. Pathol.* **58**, 515–519.

Diep, D.B., Hoen, N., Backman, M., Machon, O. & Krauss, S. (2004) Characterisation of the Wnt antagonists and their response to conditionally activated Wnt signalling in the developing mouse forebrain. *Brain Res. Dev. Brain Res.* **153**, 261–270.

Fjeld, K., Kettunen, P., Furmanek, T., Kvinnsland, I.H. & Luukko, K. (2005) Dynamic expression of Wnt signaling-related Dickkopf1, -2, and -3 mRNAs in the developing mouse tooth. *Dev. Dyn.* **233**, 161–166.

Fong, D., Hermann, M., Untergasser, G., Pirkebner, D., Draxl, A., Heitz, M., Moser, P., Margreiter, R., Hengster, P. & Amberger, A. (2009) Dkk-3 expression in the tumor endothelium: a novel prognostic marker of pancreatic adenocarcinomas. *Cancer Sci.* **100**, 1414–1420.

Guder, C., Pinho, S., Nacak, T.G., Schmidt, H.A., Hobmayer, B., Niehrs, C. & Holstein, T.W. (2006) An ancient Wnt-Dickkopf antagonism in Hydra. *Development* **133**, 901–911.

Hermann, M., Pirkebner, D., Draxl, A., Berger, P., Untergasser, G., Margreiter, R. & Hengster, P. (2007) Dickkopf-3 is expressed in a subset of adult human pancreatic beta cells. *Histochem. Cell Biol.* **127**, 513–521.

Hoang, B.H., Kubo, T., Healey, J.H., Yang, R., Nathan, S.S., Kolb, E.A., Mazza, B., Meyers, P.A. & Gorlick, R. (2004) Dickkopf 3 inhibits invasion and motility of Saos-2 osteosarcoma cells by modulating the Wnt-beta-catenin pathway. *Cancer Res.* **64**, 2734–2739.

Ishiyama, T., Kano, J., Minami, Y., Iijima, T., Morishita, Y. & Noguchi, M. (2003) Expression of HNFs and C/EBP alpha is correlated with immunocytochemical differentiation of cell lines derived from human hepatocellular carcinomas, hepatoblastomas and immortalized hepatocytes. *Cancer Sci.* **94**, 757–763.

Jung, I.L., Kang, H.J., Kim, K.C. & Kim, I.G. (2010) Knockdown of the Dickkopf 3 gene induces apoptosis in a lung adenocarcinoma. *Int. J. Mol. Med.* **26**, 33–38.

Kano, J., Ishiyama, T., Iijima, T., Morishita, Y., Murata, S., Hisakura, K., Ohkohchi, N. & Noguchi, M. (2008) Differentially expressed genes in a porcine adult hepatic stem-like cell line and their expression in developing and regenerating liver. *Lab. Invest.* **88**, 132–143.

Katase, N., Lefeuvre, M., Tsujigiwa, H., Fujii, M., Ito, S., Tamamura, R., Buery, R.R., Gunduz, M. & Nagatsuka, H. (2013) Knockdown of Dkk-3 decreases cancer cell migration and invasion independently of the Wnt pathways in oral squamous cell carcinoma-derived cells. *Oncol. Rep.* **29**, 1349–1355.

Kawano, Y., Kitaoka, M., Hamada, Y., Walker, M.M., Waxman, J. & Kypta, R.M. (2006) Regulation of prostate cell growth and morphogenesis by Dickkopf-3. *Oncogene*, **25**, 6528–6537.

Kawano, Y. & Kypta, R. (2003) Secreted antagonists of the Wnt signalling pathway. *J. Cell Sci.* **116**, 2627–2634.

Khambata, R.S., Ghosh, S.M. & Ahluwalia, A. (2015) "Repurposing" of xanthine oxidoreductase as a nitrite reductase: a new paradigm for therapeutic targeting in hypertension. *Antioxid. Redox Signal.* **23**, 340–353.

Kobayashi, K., Ouchida, M., Tsuji, T., Hanafusa, H., Miyazaki, M., Namba, M., Shimizu, N. & Shimizu, K. (2002) Reduced expression of the REIC/Dkk-3 gene by promoter-hypermethylation in human tumor cells. *Gene* **282**, 151–158.

Koppen, A., Ait-Aissa, R., Koster, J., Ora, I., Bras, J., van Sluis, P.G., Caron, H., Versteeg, R. & Valentijn, L.J. (2008) Dickkopf-3 expression is a marker for neuroblastic tumor maturation and is down-regulated by MYCN. *Int. J. Cancer* **122**, 1455–1464.

Krupnik, V.E., Sharp, J.D., Jiang, C. *et al.* (1999) Functional and structural diversity of the human Dickkopf gene family. *Gene* **238**, 301–313.

Mao, B., Wu, W., Li, Y., Hoppe, D., Stannek, P., Glinka, A. & Niehrs, C. (2001) LDL-receptor-related protein 6 is a receptor for Dickkopf proteins. *Nature* **411**, 321–325.

Muhlmann, G., Untergasser, G., Zitt, M., Zitt, M., Maier, H., Mikuz, G., Kronberger, I.E., Haffner, M.C., Gunsilius, E. & Ofner, D. (2010) Immunohistochemically detectable

 © 2017 Molecular Biology Society of Japan and John Wiley & Sons Australia, Ltd

dickkopf-3 expression in tumor vessels predicts survival in gastric cancer. *Virchows Arch.* **456**, 635–646.

Nakamura, R.E., Hunter, D.D., Yi, H., Brunken, W.J. & Hackam, A.S. (2007) Identification of two novel activities of the Wnt signaling regulator Dickkopf 3 and characterization of its expression in the mouse retina. *BMC Cell Biol.* **8**, 52.

Nie, X. (2005) Dkk1, -2, and -3 expression in mouse craniofacial development. *J. Mol. Arch.* **36**, 367–372.

Niehrs, C. (2006) Function and biological roles of the Dickkopf family of Wnt modulators. *Oncogene* **25**, 7469–7481.

Nishino, T., Nakanishi, S., Okamoto, K., Mizushima, J., Hori, H., Iwasaki, T., Nishino, T., Ichimori, K. & Nakazawa, H. (1997) Conversion of xanthine dehydrogenase into oxidase and its role in reperfusion injury. *Biochem. Soc. Trans.* **25**, 783–786.

Noguchi, M. & Hirohashi, S. (1996) Cell lines from non-neoplastic liver and hepatocellular carcinoma tissue from a single patient. *In Vitro Cell. Dev. Biol. Anim.* **32**, 135–137.

Pei, Y., Kano, J., Iijima, T., Morishita, Y., Inadome, Y. & Noguchi, M. (2009) Overexpression of Dickkopf 3 in hepatoblastomas and hepatocellular carcinomas. *Virchows Arch.* **454**, 639–646.

Roman-Gomez, J., Jimenez-Velasco, A., Agirre, X., Castillejo, J.A., Navarro, G., Barrios, M., Andreu, E.J., Prosper, F., Heiniger, A. & Torres, A. (2004) Transcriptional silencing of the Dickkopfs-3 (Dkk-3) gene by CpG hypermethylation in acute lymphoblastic leukaemia. *Br. J. Cancer* **91**, 707–713.

Sato, H., Suzuki, H., Toyota, M., Nojima, M., Maruyama, R., Sasaki, S., Takagi, H., Sogabe, Y., Sasaki, Y., Idogawa, M., Sonoda, T., Mori, M., Imai, K., Tokino, T. & Shinomura, Y. (2007) Frequent epigenetic inactivation of DICKKOPF family genes in human gastrointestinal tumors. *Carcinogenesis* **28**, 2459–2466.

St Croix, B., Rago, C., Velculescu, V., Traverso, G., Romans, K.E., Montgomery, E., Lal, A., Riggins, G.J., Lengauer, C., Vogelstein, B. & Kinzler, K.W. (2000) Genes expressed in human tumor endothelium. *Science* **289**, 1197–1202.

Suwa, T., Chen, M., Hawks, C.L. & Hornsby, P.J. (2003) Zonal expression of dickkopf-3 and components of the Wnt signalling pathways in the human adrenal cortex. *J. Endocrinol.* **178**, 149–158.

Untergasser, G., Steurer, M., Zimmermann, M., Hermann, M., Kern, J., Amberger, A., Gastl, G. & Gunsilius, E. (2008) The Dickkopf-homolog 3 is expressed in tumor endothelial cells and supports capillary formation. *Int. J. Cancer* **122**, 1539–1547.

Veeck, J., Bektas, N., Hartmann, A., Kristiansen, G., Heindrichs, U., Knuchel, R. & Dahl, E. (2008) Wnt signalling in human breast cancer: expression of the putative Wnt inhibitor Dickkopf-3 (DKK3) is frequently suppressed by promoter hypermethylation in mammary tumours. *Breast Cancer Res.* **10**, R82.

Veeck, J. & Dahl, E. (2012) Targeting the Wnt pathway in cancer: the emerging role of Dickkopf-3. *Biochim. Biophys. Acta* **1825**, 18–28.

Wang, K., Zhang, Y., Li, X., Chen, L., Wang, H., Wu, J., Zheng, J. & Wu, D. (2008) Characterization of the Kremen-binding site on Dkk1 and elucidation of the role of Kremen in Dkk-mediated Wnt antagonism. *J. Biol. Chem.* **283**, 23371–23375.

Xu, P., LaVallee, P. & Hoidal, J.R. (2000) Repressed expression of the human xanthine oxidoreductase gene. E-box and TATA-like elements restrict ground state transcriptional activity. *J. Biol. Chem.* **275**, 5918–5926.

Xu, P., LaVallee, P.A., Lin, J.J. & Hoidal, J.R. (2004) Characterization of proteins binding to E-box/Ku86 sites and function of Ku86 in transcriptional regulation of the human xanthine oxidoreductase gene. *J. Biol. Chem.* **279**, 16057–16063.

Yue, W., Sun, Q., Dacic, S., Landreneau, R.J., Siegfried, J.M., Yu, J. & Zhang, L. (2008) Downregulation of Dkk3 activates beta-catenin/TCF-4 signaling in lung cancer. *Carcinogenesis* **29**, 84–92.

Zenzmaier, C., Hermann, M., Hengster, P. & Berger, P. (2012) Dickkopf-3 maintains the PANC-1 human pancreatic tumor cells in a dedifferentiated state. *Int. J. Oncol.* **40**, 40–46.

Zenzmaier, C., Sampson, N., Plas, E. & Berger, P. (2013) Dickkopf-related protein 3 promotes pathogenic stromal remodeling in benign prostatic hyperplasia and prostate cancer. *Prostate* **73**, 1441–1452.

Received: 8 September 2016
Accepted: 7 February 2017

Supporting Information

Additional Supporting Information may be found online in the supporting information tab for this article:

Figure S1 Cell proliferation and poly (ADP-ribose) polymerase (PARP) cleavage analysis in cells transfected with another siRNA against DKK3 (siDKK3#2).

Figure S2 H_2O_2 resistance in cells with DKK3 forced overexpression with another expression vector.

Figure S3 H_2O_2-induced apoptosis in Li21 and tPH5CH cells.

Figure S4 Effects of *DKK3* knockdown on redox-related enzyme expression.

Figure S5 Relationship between Catalase (*CAT*) and *DKK3* expression in Li21 cells.

Figure S6 Effects of *DKK3* knockdown on NOX enzyme expression and activation in Li21 cells.

Table S1 Primer sequences using real-time PCR.

Table S2 cDNA microarrays in $Li21^{DKK3}$ and $tPH5CH^{DKK3}$ cells with and without H_2O_2 treatment.

© 2017 Molecular Biology Society of Japan and John Wiley & Sons Australia, Ltd